Control of grain orientation and its impact on carrier mobility in reactively sputtered Cu_2O thin films

Sanggil Han* and Andrew J. Flewitt

Electrical Engineering Division, Cambridge University, 9 JJ Thomson Avenue, CB3 0FA, Cambridge, United Kingdom

***Corresponding author: Sanggil Han**

Tel: +44 (0) 1223 762412

Email: sh810@cam.ac.uk

Address: Electrical Engineering Division, Cambridge University, 9 JJ Thomson Avenue, CB3 0FA, Cambridge, United Kingdom

Control of grain orientation and its impact on carrier mobility in reactively sputtered Cu_2O thin films

Sanggil Han[a)] and Andrew J. Flewitt

Electrical Engineering Division, Cambridge University, 9 JJ Thomson Avenue, CB3 0FA, Cambridge, United Kingdom

Abstract

Grain orientation can be particularly important in devices such as thin film transistors (TFTs) where grain boundaries present a barrier to lateral carrier transport. This paper demonstrates that thin films of nanocrystalline cuprous oxide (Cu_2O) can be grown with control of the grain orientation in the direction of either [111] or [100] perpendicular to the substrate surface using a high target utilization sputtering system. This allows a systematic study of the effect of grain orientation on the carrier mobility in Cu_2O films. It is shown that the carrier mobility in as-deposited films is similar for both grain orientations while [100]-oriented thin films exhibit a higher carrier mobility for lateral conduction than films with a [111] orientation after annealing, which is discussed from the viewpoint of the Urbach energy, crystallinity and surface morphology. This experimental finding suggests that Cu_2O thin films with a [100]

surface grain orientation are favorable for device applications such as p-type TFTs where a high in-plane carrier mobility is desired.

Keywords: p-type metal oxide, Cuprous oxide, Sputtering, Carrier mobility, Grain orientation

1. Introduction

Cuprous oxide (Cu_2O) has been proposed as a suitable channel layer for p-type metal oxide thin film transistors (TFTs) since effective hole transport is expected due to its unique orbital configuration. To be specific, energy levels of the Cu 3*d* and O 2*p* orbitals are comparable in Cu_2O, which leads to considerable covalency in the ionic metal-oxygen bonds. This results in not only a large dispersion near the top of the valence band but also a considerable reduction in the localization of holes by O 2*p* orbitals, leading to effective carrier transport [1–3]. However, actual nanocrystalline Cu_2O thin films have grain boundaries with a high degree of structural disorder (i.e. many trap states), and therefore lateral carrier transport is significantly degraded by grain boundary scattering and carrier trapping at trap states [4]. Our previous report demonstrated that vacuum annealing can be used to improve the low carrier mobility in Cu_2O films without phase conversion to either CuO or Cu [5].

Grain orientation can also affect the carrier mobility in Cu_2O films where grain boundaries impede carrier transport. Most of the existing literature on control of the Cu_2O

grain orientation is based on the electrodeposition method and it was shown that the grain orientation is controlled by its several deposition parameters (e.g. electrolyte pH and potential applied to the electrode) [6–10]. However, the conductive substrate required for electrodeposition causes difficulty in accurately measuring electrical characteristics of a Cu_2O film itself, which hinders a systematic investigation into the effect of grain orientation on the carrier mobility. This can be easily solved through control of the grain orientation by vacuum process techniques (e.g. reactive sputtering and chemical vapor deposition) enabling the use of an insulating substrate such as glass.

Films generally tend to grow with the crystalline plane of the lowest surface energy parallel to the substrate surface to minimize the surface energy [11,12]. It was found that an increase in adatom mobility enables the growth of crystalline planes different from that of the lowest surface energy [12–14]. In the case of Cu_2O, the nonpolar (111) plane was demonstrated to have the lowest surface energy E_S (0.677 $J \cdot m^{-2}$) [15]. Based on the surface energy consideration alone, Cu_2O films are expected to have the [111] preferred grain orientation. Wang *et al*. showed that the preferred orientation in sputtered Cu_2O films can be changed from the [111] direction to the [100] direction (which has a significantly higher surface energy of 1.194 $J \cdot m^{-2}$ [15]) by an increase in adatom mobility through adjusting the process pressure [14]. In addition to the process pressure, the ion-to-metal flux ratio (J_i/J_{me}) incident at the growing film during sputter deposition is known to be a control parameter for the kinetic energy of adatoms (i.e. adatom mobility) [16,17]. For example, an increase in J_i/J_{me} leads to an increase in the number of energetic ions which collides with each metal

adatom at the growing film surface, which results in an increase in ion-adatom momentum transfer (i.e. higher adatom mobility).

A high target utilization sputtering (HiTUS) system (Plasma Quest Limited) enables a precise control of J_i/J_{me} through simply adjusting the ion current (i_C) which is a sputtering parameter related to an Ar plasma density at the surface of a metal target (see a detailed description and a schematic diagram of HiTUS in Ref [18]). Specifically, in the case of reactive sputtering of Cu_2O, the ion flux (J_i) incident at the growing film mainly consists of the ions generated by the Ar and O_2 plasma near to the grounded substrate holder. An increased i_C means an increase in the Ar plasma density at the Cu target surface, which leads to more Cu atoms being emitted from the target (i.e. a higher Cu flux, J_{Cu}). On the other hand, the change in i_C has a negligible effect on the Ar plasma density near to the growing film and the O_2 plasma remains constant by using the same oxygen flow rate, which allows the assumption of a constant J_i. Therefore, an increase in i_C results in a reduction in J_i/J_{Cu} (i.e. i_C is inversely related to J_i/J_{Cu}).

In this letter, it is demonstrated that Cu_2O films can be grown with control of the grain orientation in the direction of either [111] or [100] perpendicular to the substrate surface through adjusting i_C of the HiTUS system. This allows an investigation to determine which one of the two grain orientations is more favorable in terms of the in-plane carrier mobility. Furthermore, the impact of grain orientation on the carrier mobility in both as-deposited and annealed films of Cu_2O is discussed based on the Urbach energy, crystallinity and surface morphology.

2. Experimental Details

Cu_2O thin films were deposited by the HiTUS system from a metallic Cu target with 4-inch diameter and 99.999% purity (Kurt J. Lesker Company) in an Ar/O_2 gas mixture (99.9995% purity; BOC Gases Ltd). The base pressure in the chamber was 6.0×10^{-4} Pa, and Ar gas was provided to set a process pressure of 1.5×10^{-1} Pa. The reactive sputtering was performed at a constant DC bias voltage (a sputtering parameter related to ion energy, E_i) of 690 V and an oxygen flow rate of 16 sccm without intentional substrate heating. i_C was varied from 1.38 A to 1.52 A in order to investigate the J_i/J_{Cu} dependence on the Cu_2O grain orientation. Surface profilometry (Veeco Dektak 200SI) was used to measure film thickness. The film thickness increased from 500 to 550 nm with an increase in i_C from 1.38 to 1.52 A. The films were annealed at various temperatures (500, 600 and 700 °C) for 10 min in vacuum (9.5×10^{-2} Pa) in an Aixtron Cambridge Nanoinstruments Black Magic 2 system. An infrared (IR) radiation pyrometer (Infratherm IGA8 plus) was used for monitoring the annealing temperature. The temperature ramp rate was 5 K s^{-1} and all the annealed films were unloaded at a chamber temperature of 50 °C. Four Au electrodes were formed at the corners of the Cu_2O films deposited on 8 mm × 8 mm glass (Corning 7059) substrates using a thermal evaporator (Edwards E306A) and a shadow mask in order to measure Hall mobility (μ_{Hall}) using the van der Pauw method.

In order to check grain orientation of Cu_2O thin films, X-ray diffraction (XRD) patterns were obtained using a Bruker D8 Discover X-ray diffractometer with the following measurement set-up: Cu $K_{\alpha1}$ X-ray source with a wavelength of 0.154 nm, X-ray generator

power (40 kV and 40 mA), monochromator slit size (0.2 mm) and scan speed (1.5 sec/step). μ_{Hall} was obtained based on the conventional measuring standard in the van der Pauw configuration using an MMR Technologies Hall Effect Measurement System (K2500-7) at room temperature. Specifically, thermoelectric and misalignment offsets are corrected by reversing the direction of current flow and magnetic field, and then μ_{Hall} is determined by averaging the corrected Hall voltages along the two diagonals of the sample. Furthermore, a Hall scattering factor ($1 \leq r \leq 2$) reflecting intrinsic scattering mechanisms in single crystals or grains was approximated to be $r = 1$ in the μ_{Hall} calculations since the μ_{Hall} values are used for the purpose of comparing an apparent mobility including the grain boundary effect, not a true in-grain carrier mobility, between the [111] and [100] oriented films. The optical absorption coefficient ($\alpha(\upsilon)$) was obtained by an ATI Unicam UV/Vis spectrometer (UV2-200) to extract the Urbach energy (E_u), and scanning electron microscope (SEM) images were taken using a LEO GEMINI 1530VP FEG-SEM system with an operating voltage of 3 kV.

3. Results and Discussion

The XRD patterns of Cu_2O films grown at different i_C values are shown in Fig. 1. The Cu_2O (111) peak is detected for $i_C \geq 1.5$ A (a lower J_i/J_{Cu}), while the intense peak related to the Cu_2O (200) plane is observed for $i_C < 1.5$ A (a higher J_i/J_{Cu}). On the basis of the evolutionary selection theory based on the growth rate anisotropy of the different crystalline planes [12,19], it is proposed that for $i_C < 1.5$ A (i.e. a higher J_i/J_{Cu}), the grains with the (200) plane parallel to the substrate surface would grow faster and at the expense of those (with the

(111) plane parallel to the surface) grown by a slower vertical growth rate, and this results in the [100] preferred grain orientation despite its relatively higher surface energy. Given that an increase in J_i/J_{Cu} leads to a higher adatom mobility, this result is consistent with the work of Wang showing that the [100] preferred orientation with high surface energy can be obtained by an increase in adatom mobility [14]. In addition, contrary to a gradual transition of preferred grain orientation in polycrystalline TaN films from [111] to [111] + [001] and to complete [001] with an increase in J_i/J_{Ta} [20], Cu_2O films grown by the HiTUS system show an abrupt transition between [111] and [100] as seen in Fig. 1.

In order to investigate the grain orientation effect on the in-plane carrier mobility in Cu_2O films, the samples grown at i_C = 1.38 A and i_C = 1.52 A were selected as the [100] and [111]-oriented films, respectively, and μ_{Hall} of the as-deposited and annealed films was measured as seen in Fig. 2. This shows that both as-deposited films exhibit a similar μ_{Hall}, but a distinct difference in the extent of mobility enhancement appears as a result of annealing with the [100]-oriented film showing a more significant enhancement of μ_{Hall}. The [100]-oriented film annealed at 700 °C shows a μ_{Hall} of 28 $cm^2/V{\cdot}s$ which is one of the highest values obtained by sputtered copper oxide films [21–23].

Based on the assumption that Cu_2O has a perfect single crystal structure, the effective mass for the light hole band situated at the top of the valence band was found to be isotropic by density functional theory calculations [24]. This means that a defect-free Cu_2O grain is expected to have the same carrier mobility regardless of its crystallographic orientation. However, a nanocrystalline Cu_2O film has grain boundaries with a high degree of structural

disorder causing many defects, which impedes lateral carrier transport. It is well-known that Urbach energy (E_u) is a measure of structural disorder [25,26], and in polycrystalline films, it is assumed that E_u is caused by several factors such as strain and bulk and grain boundary carrier trapping [27]. A theoretical analysis indicated that the disorder distribution is gradual with a maximum close to the grain boundary and decreases toward the center of the grain [28]. Furthermore, an inverse correlation between E_u and grain size is widely observed [21, 28]. Both theoretical and experimental results indicate that the grain boundary is the main source of disorder in polycrystalline films. For this reason, the level of structural disorder in the films is compared by E_u extracted using the following method in order to interpret the μ_{Hall} results.

The optical absorption tail follows the empirical exponential law represented by $\alpha(\upsilon) = \alpha_0 \exp(h\upsilon/E_u)$, where α, α_0, h and υ denote the optical absorption coefficient, a constant, the Planck constant and the photon frequency, respectively [29,30]. This equation can be expressed as $\ln(\alpha) = (1/E_u)(h\upsilon) - \ln(\alpha_0)$, and therefore E_u can be extracted from the reciprocal of the slope of the linear region in the $\ln(\alpha)$ versus $h\upsilon$ (i.e. photon energy) plot as seen in Fig. 3a. The extracted E_u values of the [111] and [100]-oriented Cu_2O films are shown in Fig. 3b as a function of annealing temperature, which provides an insight into the μ_{Hall} results. The similar μ_{Hall} in the as-deposited films can be explained by the isotropic hole effective mass (i.e. the same mobility in defect-free grains in the direction of [100] and [111]) and a similar E_u (i.e. a similar degree of disorder in the films). The more significant enhancement of μ_{Hall} in the [100]-oriented film after annealing is considered to be due to a more considerable

reduction of disorder in the film than that in the [111]-oriented film based on the extracted E_u.

In order to identify the main cause of the more significant reduction in disorder in the [100]-oriented film, the crystallographic characteristics and surface morphology of the 700 °C-annealed films were investigated by XRD and SEM. The XRD patterns (Fig. 4) of the [111] and [100]-oriented films annealed at 700 °C were obtained from the same XRD system and measurement set-up as described in section 2 (Experimental Details). This clearly shows that the intensity (I) of the diffraction peak of the [100]-oriented Cu_2O film increases much more significantly after annealing ($I_{(200)}$: 95 counts per second (cps) (as-deposited) → 4175 cps (700 °C), $I_{(111)}$: 188 cps (as-deposited) → 298 cps (700 °C)). This indicates that the crystallinity of the [100]-oriented film improves more considerably than that of the [111]-oriented film after annealing. In addition, it is observed that the (111) peak of the [111]-oriented Cu_2O film shifts from 36.74° (as-deposited) to 36.46° (700 °C) which is closer to the reference peak of 36.44° [JCPDS 04-007-9767]. This can be explained by the release of the compressive stress in the film by annealing considering the fact that the compressive stress gives rise to a reduction in the lattice constant and this in turn results in a shift of its diffraction peak to a higher angle on the basis of Bragg's law. The SEM images (Fig. 5) show an interesting outcome that grains in the [100]-oriented film seem to be completely coalesced by annealing of 700 °C contrary to those in the [111]-oriented film. This experimental result suggests that the [100] texture with a higher surface energy is favorable for grain growth (i.e. grain coalescence) by annealing. This is considered to be the main reason for the more

significant improvement in crystallinity and greater reduction in disorder in the [100]-oriented film compared to the [111]-oriented film after annealing, which in turn results in a much higher carrier mobility in the [100]-oriented film.

4. Conclusions

It was demonstrated that the grain orientation in Cu_2O films can be controlled in the direction of either [111] or [100] by a change in adatom mobility through adjusting the ion current (i.e. the ion-to-Cu flux ratio (J_i/J_{Cu}) incident at the growing film) using the HiTUS technique. To be specific, a low J_i/J_{Cu} leads to the growth of nanocrystalline Cu_2O films with the [111] surface orientation which has the lowest surface energy, while an increase in J_i/J_{Cu} yields Cu_2O films with the [100] orientation of the highest surface energy. In addition, a systematic study on the grain orientation effect on the in-plane carrier mobility in Cu_2O films was performed. This shows that as-deposited films exhibit a similar carrier mobility for both grain orientations due to an isotropic hole effective mass and a similar degree of disorder in the films. By contrast, after annealing, the [100]-oriented film shows a more significant improvement in the carrier mobility due to a greater reduction in the degree of disorder in the film. Lastly, the [100] texture with a higher surface energy was found to be favorable for grain coalescence by annealing, which provides an insight into the higher crystallinity and lower degree of disorder in the [100]-oriented film after annealing. These experimental results suggest that the [100] preferred texture is favorable for device applications such as p-type metal oxide TFTs requiring a high in-plan carrier mobility.

Acknowledgements

This work was supported by the Engineering and Physical Sciences Research Council under Grant No. EP/M013650/1. Additional data related to this publication is available at the DSpace@Cambridge data repository (http://www.repository.cam.ac.uk).

References

[1] H. Raebiger, S. Lany, A. Zunger, Origins of the p-type nature and cation deficiency in Cu_2O and related materials, Phys. Rev. B 76 (2007) 045209. https://doi.org/10.1103/PhysRevB.76.045209.

[2] H. Kawazoe, H. Yanagi, K. Ueda, H. Hosono, Transparent *p*-Type conducting oxides: Design and fabrication of *p-n* heterojunctions, MRS Bull. 25 (2000) 28–36. https://doi.org/10.1557/mrs2000.148.

[3] H. Yanagi, H. Kawazoe, A. Kudo, M. Yasukawa, H. Hosono, Chemical design and thin film preparation of *p*-Type conductive transparent oxides, J. Electroceram. 4 (2000) 407–414. https://doi.org/10.1023/A:1009959920435.

[4] S. Han, A.J. Flewitt, Analysis of the conduction mechanism and copper vacancy density in p-type Cu_2O thin films, Sci. Rep. 7 (2017) 5766. https://doi.org/10.1038/s41598-017-05893-x.

[5] S. Han, K.M. Niang, G. Rughoobur, A.J. Flewitt, Effects of post-deposition vacuum annealing on film characteristics of p-type Cu_2O and its impact on thin film transistor characteristics, Appl. Phys. Lett. 109 (2016) 173502. https://doi.org/10.1063/1.4965848.

[6] T.D. Golden, M.G. Shumsky, Y. Zhou, R.A. VanderWerf, R.A. Van Leeuwen, J.A. Switzer, Electrochemical Deposition of Copper(I) Oxide Films, Chem. Mater. 8 (1996) 2499-2504. https://doi.org/10.1021/cm9602095.

[7] L.C. Wang, N.R. de Tacconi, C.R. Chenthamarakshan, K. Rajeshwar, M. Tao, Electrodeposited copper oxide films: Effect of bath pH on grain orientation and orientation-dependent interfacial behavior, Thin Solid Films 515 (2007) 3090–3095. https://doi.org/10.1016/j.tsf.2006.08.041.

[8] S. Bijani, L. Martínez, M. Gabás, E.A. Dalchiele, J.R. Ramos-Barrado, Low-temperature electrodeposition of Cu_2O thin films: modulation of micro-nanostructure by modifying the applied potential and electrolytic bath pH, J. Phys. Chem. C 113 (2009) 19482–19487. https://doi.org/10.1021/jp905952a.

[9] W. Wu, K. Feng, B. Shan, N. Zhang, Orientation and grain shape control of Cu_2O film and the related properties, Electrochimica Acta 176 (2015) 59–64. https://doi.org/10.1016/j.electacta.2015.06.010.

[10] C. Wang, J. Xu, S. Shi, Y. Zhang, Z. Liu, X. Zhang, S. Yina, L. Li, Structural, optical and photoelectrical properties of Cu_2O films electrodeposited at different pH, RSC Adv. 6 (2016) 4422–4428. https://doi.org/10.1039/C5RA23216C.

[11] R. Banerjee, R. Chandra, P. Ayyub, Influence of the sputtering gas on the preferred orientation of nanocrystalline titanium nitride thin films, Thin Solid Films 405 (2002) 64–72. https://doi.org/10.1016/S0040-6090(01)01705-9.

[12] S. Nicolay, S. Fay, C. Ballif, Growth model of MOCVD polycrystalline ZnO, Cryst. Growth Des. 9 (2009) 4957–4962. https://doi.org/10.1021/cg900732h.

[13] L. Fanni, A.B. Aebersold, M. Morales-Masis, D.T.L. Alexander, A. Hessler-Wyser, S. Nicolay, C. Hébert, C. Ballif, Increasing polycrystalline zinc oxide grain size by control

of film preferential orientation, Cryst. Growth Des. 15 (2015) 5886–5891. https://doi.org/10.1021/acs.cgd.5b01299.

[14] Y. Wang, J. Ghanbaja, F. Soldera, S. Migot, P. Boulet, D. Horwat, F. Muecklich, J.-F. Pierson, Tuning the structure and preferred orientation in reactively sputtered copper oxide thin films, Appl. Surf. Sci. 335 (2015) 85–91. https://doi.org/10.1016/j.apsusc.2015.02.028.

[15] Z. Zheng, B. Huang, Z. Wang, M. Guo, X. Qin, X. Zhang, P. Wang, Y. Dai, Crystal faces of Cu_2O and their stabilities in photocatalytic reactions, J. Phys. Chem. C 113 (2009) 14448–14453. https://doi.org/10.1021/jp904198d.

[16] L. Hultman, J.-E. Sundgren, J.E. Greene, D.B. Bergstrom, I. Petrov, High-flux low-energy (20 eV) N_2^+ ion irradiation during TiN deposition by reactive magnetron sputtering: Effects on microstructure and preferred orientation, J. Appl. Phys. 78 (1995) 5395–5403. https://doi.org/10.1063/1.359720.

[17] D. Gall, S. Kodambaka, M.A. Wall, I. Petrov, J.E. Greene, Pathways of atomistic processes on TiN(001) and (111) surfaces during film growth: an ab initio study, J. Appl. Phys. 93 (2003) 9086–9094. https://doi.org/10.1063/1.1567797.

[18] A.J. Flewitt, J.D. Dutson, P. Beecher, D. Paul, S.J. Wakeham, M.E. Vickers, C. Ducati, S.P. Speakman, W.I. Milne, M.J. Thwaites, Stability of thin film transistors incorporating a zinc oxide or indium zinc oxide channel deposited by a high rate sputtering process, Semicond. Sci. Technol. 24 (2009) 085002. http://dx.doi.org/10.1088/0268-1242/24/8/085002.

[19] A. van der Drift, Evolutionary selection, a principle governing growth orientation in vapour-deposited layers, Phillips Res. Rep. 22 (1967) 267–288.

[20] I. Petrov, P.B. Barna, L. Hultman, J.E. Greene, Microstructural evolution during film growth, J. Vac. Sci. Technol. A 21 (2003) S117–S128. https://doi.org/10.1116/1.1601610.

[21] Y. Wang, P. Miska, D. Pilloud, D. Horwat, F. Mucklich, J. F. Pierson, Transmittance enhancement and optical band gap widening of Cu_2O thin films after air annealing. J. Appl. Phys. 115 (2014) 073505. http://dx.doi.org/10.1063/1.4865957.

[22] E.-S. Cho, J. Sohn, S.-H. Song, H.-I. Kwon, Active layer thickness effects on the structural and electrical properties of p-type Cu_2O thin-film transistors, J. Vac. Sci. Technol. B 30 (2012) 060605. https://doi.org/10.1116/1.4764110.

[23] K.C. Sanal, L.S. Vikas, M.K. Jayaraj, Room temperature deposited transparent p-channel CuO thin film transistors, Appl. Surf. Sci. 297 (2014) 153–157. https://doi.org/10.1016/j.apsusc.2014.01.109.

[24] X. Nie, S.-H. Wei, S.B. Zhang, First-principles study of transparent *p*-type conductive $SrCu_2O_2$ and related compounds, Phys. Rev. B 65 (2002) 075111. https://doi.org/10.1103/PhysRevB.65.075111.

[25] D. Nesheva, Z. Levi, Z. Aneva, V. Nikolova, H. Hofmeister, Experimental studies on the defect states at the interface between nanocrystalline CdSe and amorphous SiOx, J. Phys.: Condens. Matter. 12 (2000) 751–759.

[26] S. Ahmad, K. Asokan, M. Zulfequar, Investigation of structural and optical properties of 100 MeV F^{7+} ion irradiated $Ga_{10}Se_{90-x}Al_x$ thin films, Philos. Mag. 95 (2015) 1309–1320. https://doi.org/10.1080/14786435.2015.1023860S0953-8984(00)05981-6.

[27] D. Dragoman, M. Dragoman, Optical Characterization of Solids, first ed., Springer, Heidelberg, 2002

[28] A. Iribarren, R. Castro-Rodriguez, F. Caballero-Briones, J. L. Pena, Optical and structural evidence of the grain-boundary influence on the disorder of polycrystalline CdTe films, Appl. Phys. Lett. 74 (1999) 2957–2959. https://doi.org/10.1063/1.123978.

[29] Y. Natsume, H. Sakata, T. Hirayama, Low-temperature electrical conductivity and optical absorption edge of ZnO films prepared by chemical vapour deposition, Phys. Status Solidi A 148 (1995) 485–495. https://doi.org/10.1002/pssa.2211480217.

[30] S.J. Ikhmayies, R.N. Ahmad-Bitar, A study of the optical bandgap energy and Urbach tail of spray-deposited CdS:In thin films, J. Mater. Res. Technol. 2 (2013) 221–227. https://doi.org/10.1016/j.jmrt.2013.02.012.

List of figure captions

Fig. 1. X-ray diffraction patterns of Cu_2O films deposited at various ion currents. A small peak from the sample holder is also present.

Fig. 2. Hall mobility of [100] and [111]-oriented Cu_2O films as a function of annealing temperature. Inset shows a schematic van der Pauw geometry for the Hall-effect measurement.

Fig. 3. (a) ln(α) versus photon energy plots of [111] and [100]-oriented Cu_2O films with different annealing temperatures and (b) their extracted Urbach energy as a function of annealing temperature.

Fig. 4. X-ray diffraction patterns of the [100] and [111]-oriented Cu_2O films annealed at 700 °C.

Fig. 5. Scanning electron microscope images of (a) [100] and (b) [111]-oriented Cu_2O films annealed at 700 °C.

Figures

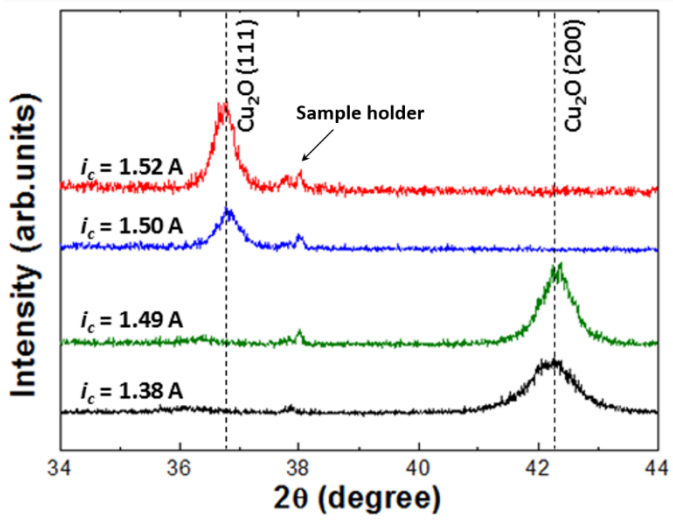

FIG. 1. X-ray diffraction patterns of Cu_2O films deposited at various ion currents. A small peak from the sample holder is also present.

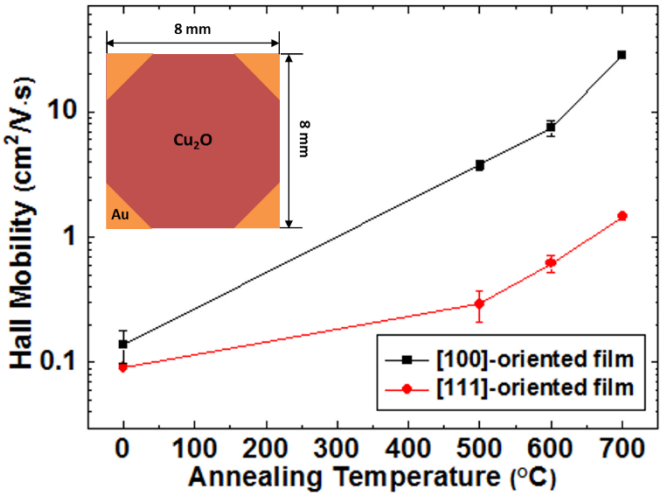

FIG. 2. Hall mobility of [100] and [111]-oriented Cu_2O films as a function of annealing temperature. Inset shows a schematic van der Pauw geometry for the Hall-effect measurement.

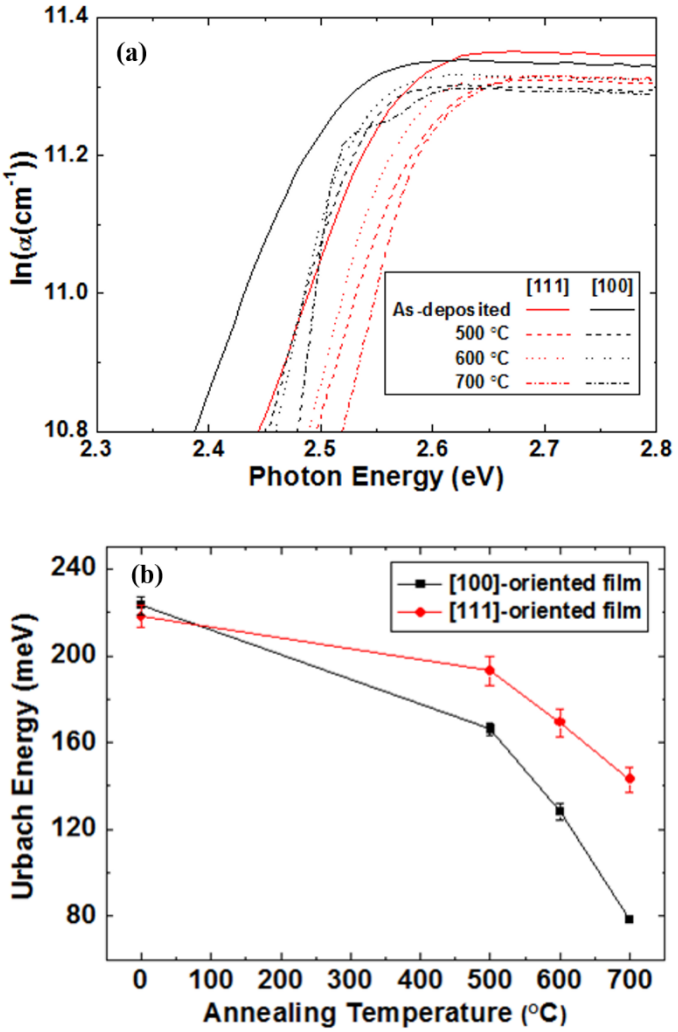

FIG. 3. (a) ln(α) versus photon energy plots of [111] and [100]-oriented Cu_2O films with different annealing temperatures and (b) their extracted Urbach energy as a function of annealing temperature.

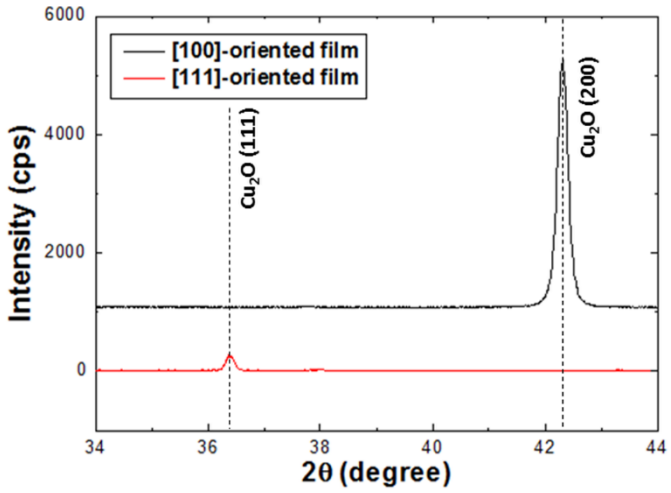

FIG. 4. X-ray diffraction patterns of the [100] and [111]-oriented Cu_2O films annealed at 700 °C.

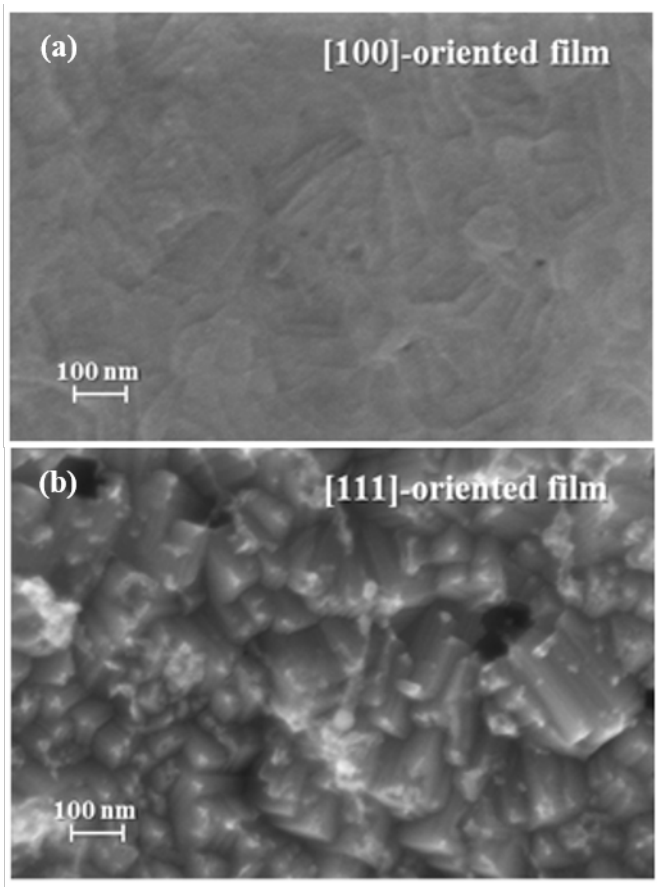

FIG. 3. Scanning electron microscope images of (a) [100] and (b) [111]-oriented Cu_2O films annealed at 700 °C.